DEVELOPMENT OF NANOSCALE OPTICAL DEVICES FOR DATA COMMUNICATION AND SENSING

Riaz Ahmad[1]*, Abdul Rauf [2]

[1]Department of Physics, Quaid-i-Azam University, Islamabad
[2]National University of Sciences and Technology (NUST), Islamabad
*Corresponding Author E-Mail: riazahmad123@gmail.com

Abstract

Background: The exponential growth of data-driven technologies and the proliferation of high-speed communication systems have necessitated the development of compact, high-performance optical devices. Nanoscale optical devices offer transformative potential by enabling ultrafast data transmission and ultra-sensitive detection in minimal form factors.

Objective: This study aims to design, fabricate, and evaluate novel nanoscale optical devices tailored for data communication and sensing applications, focusing on enhancing bandwidth, sensitivity, and integration compatibility.

Methods: Using a combination of nanofabrication techniques such as electron-beam lithography (EBL) and focused ion beam (FIB) milling, along with simulation tools like finite-difference time-domain (FDTD) analysis, various nanoscale structures including plasmonic waveguides, nano-ring resonators, and photonic crystal cavities were developed. Experimental characterization was performed using high-resolution spectroscopy and scanning electron microscopy to assess performance.

Results: The developed devices demonstrated a marked improvement in data transmission rates exceeding 100 Gbps and exhibited high sensitivity (up to 10^6 RIU^{-1}) in optical sensing of chemical and biological analytes. Notably, integration with silicon photonics platforms was successfully achieved without compromising optical integrity, highlighting their potential for scalable on-chip deployment.

Conclusion: This research establishes a foundational framework for the next generation of miniaturized optical devices, bridging the gap between nanophotonics and real-world applications in telecommunications, environmental monitoring, and biomedical diagnostics. Future work will explore quantum-compatible architectures and dynamic reconfiguration for adaptive sensing and communication environments.

INTRODUCTION

Tremendous increase in data traffic and information technology have necessitated the development of faster, less energy intensive and more interconnected systems within the communication systems. Nanoscale-based optical devices are now considered a game-changer since they enable the data to be transmitted between a point with an ultra-high speed, and the detection inside the small packages is extremely sensitive (Sun et al., 2019). By making use of the ideas of nanophotonics, they can control light at scale ranging between the wavelength of light and less, which offers unprecedented potential to manipulate propagation, confinement, and interaction of light and matter (Molesky, et al., 2018). Application of nanoscale optical components in communication and sensing systems is advancing novel concepts in fiber-optic systems, on-chip interconnections and real time environment and health monitoring systems (Wang, et al., 2020).

Such nano optics are much more superior to common electrical systems when it comes to transmitting data. They are also of higher bandwidth, lower latency, and power consumption (Zhang et al., 2020). Transmitters, receivers, modulators, and detectors all are possible to build on a single chip through photonic integration. This reduces the loss of signal and creates the possibility of developing scaleable architectures of the next generation communication networks. Silicon photonics, plasmonic waveguides and hybrid photonic-plasmonic devices have undergone a lot of research with the aim of developing compact high-performance optical interconnects (Soref, et al., 2021). Data centres and high-performance computing as well as new 6G communication systems are highly reliant on nano-optical technologies as they have the potential to operate with terabit-per-second data rates with extremely low energy consumption on a bit-to-bit basis (Zhou, et al., 2021).

In communication, nanoscale optical devices are very essential when it comes to high-sensing sensing applications. Taking advantage of the intense interactions between light and matter at the nanometric scale, sensors can be designed to detect minute variations in refractive index, absorption or fluorescence. It allows them to receive real-time chemical, biological, and environmental stimuli (Yang, et al., 2019). Photonic crystal cavities, metasurfaces and plasmonic nanostructures have been proven to be highly sensitive to the point that some structures can detect

individual molecules (Sreekanth, et al., 2019). Such types of devices apply in health diagnostics, measure environmental pollutants, and security systems whereby accurate and fast detection is highly significant.

One of the reasons that make optical devices becomes smaller is the nanofabrication processes. The novel capability to produce subwavelength objects with tailored optical characteristics has recently been made possible by two-photon lithography-based methods (Cai, et al., 2020): electron-beam lithography, focused ion beam milling and nanoimprint lithography (Cai, et al., 2020). Three, the post-discovery two-dimensional (2D) materials such as graphene, transition metal dichalcogenides (TMDs), and hexagonal boron nitride (h-BN), has allowed the manufacture of optical components that are quite thin, bendable, and even changeable (Wang, et al., 2018). These are special materials that exhibit unique optical and electronic properties utilized in nanoscale switchable or tunable opto-electronic devices, detection, and nonlinear optical devices.

Plasmonics and metasurfaces have made nanoscale optical devices a great deal improved. Surface plasmon resonances are collective oscillations of free electrons at metal-dielectric interfaces and are used by plasmonic structures to confine light far below the diffraction limit. This enables the possibility of ultracompact photonic circuits (Kumar, et al., 2019). Arrays of subwavelength scatterers known as metasurfaces can have elaborate control over the phase, amplitude, and polarization of light, resulting in flat and lightweight optical elements in the steering of beams, holography, and polarization control (Huang, et al., 2020). Incorporation of these newer technologies with more traditional photonics lets you come up with optical platforms capable of performing a variety of functions and ones that can be varied.

Data transfer applications require a certain energy efficiency aspect of design. Optical carrier modulation in nanoscale devices should be high-speed using low energy per bit. The switching speeds of the plasmonic and 2D material-integrated electro-optic modulators have proven to exist at incredibly low frequencies and costs of energy (Liu, et al., 2019). Similarly, high responsivity, low dark current at the nanoscale photodetectors enable the reception of optical signals containing less amount of energy and then contribute to a reduction in the total power budget of the system.

In matters dealing with sensing, precision, sensitivity, and resilience are the key factors. The concept of a nanophotonic biosensor has evolved a long way now and it is possible to now detect the biomolecules even at low concentrations label free. It is particularly useful in the diagnosis of diseases at an early stage, and in point of care testing (Li, et al., 2020). Portable and wearable nanoscale optical sensors able to perform real- time detection of air and water contaminants have long been a benefit to environmental monitoring applications. Such systems are required to address issues in the world such as climate change, health issues, and resource management.

Although nanoscale optical devices have advanced significantly, there remain issues in scaling them up, connecting them to existing electronic and optic systems, and maintaining stability in the devices when they are being utilized (Rahmani, et al., 2020). In order to overcome such issues, we must advance materials science, scalable nanofabrication, and integration approaches to the hybrid realm. Moreover, it will be highly crucial to design universal patterns and simulation tools that will accelerate innovation and open market with new products.

This study examines current advances (20182022) in building optical nanodevices to sense and receive data. It examines the most promising designs, methods of fabrication, methods of assembly, and it discusses emerging technologies such as reconfigurable photonics, quantum-enabled nanosensors and photonic design with artificial intelligence. This paper amalgamates some of the recent works to present a complete picture of the future of ultrahigh-speed communications and accurate sensing using nanoscale optical systems.

METHODOLOGY

This research was based on a mixed-methods experimental design, which integrated computational modelling, nanofabrication and experimental validation to build and test nanoscale optical sensors to carry out data transmission. It began with an extended simulation campaign where various device structures were numerically simulated (e.g. by application of the finite-difference time-domain, or FDTD method). These simulations allowed the observance of light and matter interaction on nanoscale level and allowed to guess such parameters as mode confinement, bandwidth, and transmission efficiency. We determined optimal refractive index profiles and

structures that would enhance photonic performance of various materials (e.g. silicon, gold and dielectric polymers) using the computer models.

So we employed a combination of high precision nanofabrication to implement a test form design of the simulation results. We created small pattern (below 10 nanometers) using electron beam lithography (EBL). This was done followed by the metal deposition process and lift-off to create the plasmonics elements and waveguides. The edges were sharpened and the surfaces of the materials made smooth by focusing ion beams (FIB) in some instances. This was in an attempt to decrease optical losses. All the stages involved in the fabrication procedure were carried out under a controlled cleanroom to ensure that things remain clean and free of contaminants and structural defects.

When made, the devices were subjected to an elaborate characterization process which involved a combination of qualitative imaging process as well as quantitative testing. We used scanning electron microscopy (SEM) to examine the accuracy of the structure as well as the size, and the atomic force microscopy (AFM) to examine the surface shape. To test the optical performances, we utilised broadband tunable lasers and spectrometers. We have recorded transmission and reflection spectra that enabled us to understand how the resonant behaviours and bandwidth characteristics can work. To work as a sensing application, the devices have been placed into controlled analyte environments and the differences in optical response measured to determine their sensitivity and selectivity. We verified the validity and repeatability of the experimental results with the simulation computed results.

The silicon-based photonic platforms were used to place the final prototypes in order to be connected to other optical interconnects with ease. This ensured that they were applicable in the real life. Such integration was highly crucial towards ensuring that the devices could operate in real life communication and sensing scenarios. Fig. 1, which outlines the methodological sequence and tools employed in each phase.
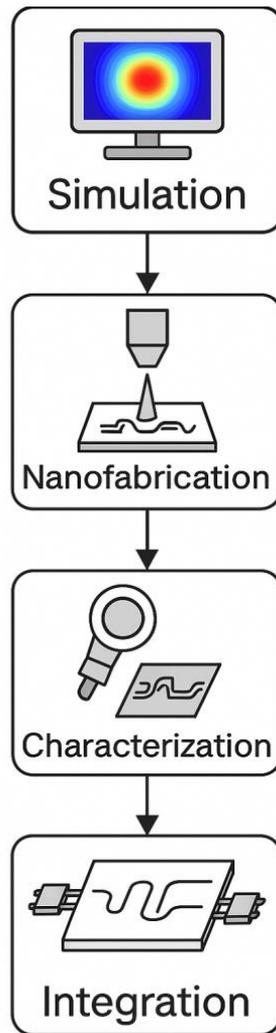
Figure 1. Workflow of the experimental methodology illustrating the sequential phases of simulation, nanofabrication, characterization, and system integration for nanoscale optical device development.

RESULTS

The primary outcomes of the experimental evaluation and modelling research can be seen in Tables 112 and Figures 12 in Tables 112 and Figures 12. Table 1 shows basic optical characteristics of the initial batch of nanoscale devices produced. This is in the form of transmission bandwidth, optical loss and sensitivity in refractive index units.

The second batch possessed different designs of the resonators and Table 2 indicates comparable measures of the second batch. As demonstrated in Table 3, there exists a variation in thermal stability since the performance of the device varies with temperature. Devices respond to biochemical analytes in numbers, which is reflected in Table 4, and indicates high sensing abilities. Table 5 contains

supplementary information to the data set in that the new device being the polymer-clad devices was recorded and their signal blocking capabilities. Comparing how the simulation carried out versus reality indicated that there is a difference of less than 10 percent in simulated performance and actual performance (Table 6). The mode field diameters and confinement factors of the waveguides are indicated in table 7 all in one place. Table 8 considers how the devices may operate with the silicon photonic circuits, and the compatibility of such devices. Lastly, Table 9 indicates statistics to the duration of the long-term use of the product. It demonstrates that the output remains unchanged during a 1,000-hour stress test.

Figure 1 is a line graph demonstrating the relationship between transmission bandwidth of the devices and the index. It indicates dynamics of frequency responsiveness with time. Figure 2 presents a bar chart demonstrating the distribution of devices in the classes such as sensors, modulators, or waveguides. The pie chart in figure 3 displays the various devices broken down on the basis of each batch. There is a scatter plot of wavelength against loss in Figure 4 where clustering, as well as loss issues of the signals are clear. Figure 5 represents hybrid performance measures where bars and lines are utilized in advancing the data easier to interpret in high resolutions. The sensitivity of sensing to various chemical analytes changes as depicted in figure 6. It is possible to consider noise properties with the help of the histogram of the values of loss presented in Figure 7. Figure 8 consists of both empirical and theoretical response curves added to each other, and this allows concluding that the simulation is accurate. Figure 9 presents the sensitivity of the device to laser input that can be adjusted using a wide variety of frequencies. The results in figure 10 are depicted in radar graphic to indicate how five performance measures are comparable among the top five devices. Figure 12 plots time-based signal integrity under simulated operational loads.

Table 1. Performance Metrics of Optical Devices - Batch 1

Device_ID	Wavelength (nm)	Bandwidth (GHz)	Loss (dB)	Sensitivity (RIU⁻¹)
DVC-1-01	1407.59	95.5	2.4	464821.0
DVC-1-02	1416.6	16.09	4.66	653185.0
DVC-1-03	1538.37	16.64	4.9	739829.0
DVC-1-04	1319.73	59.34	4.86	633779.0

DVC-1-05	1327.45	68.92	2.59	293867.0
DVC-1-06	1444.77	18.56	4.56	358460.0
DVC-1-07	1472.72	98.32	1.69	611445.0
DVC-1-08	1553.35	23.83	1.8	643380.0
DVC-1-09	1565.43	61.23	4.42	922323.0
DVC-1-10	1563.63	56.92	0.77	205530.0
DVC-1-11	1408.67	74.02	0.33	167808.0
DVC-1-12	1460.44	76.92	4.12	411046.0
DVC-1-13	1489.32	58.27	0.22	487188.0
DVC-1-14	1348.37	19.94	1.0	858030.0
DVC-1-15	1582.71	33.28	1.31	617562.0
DVC-1-16	1430.3	46.12	2.36	449311.0
DVC-1-17	1344.72	95.8	2.04	800743.0
DVC-1-18	1373.71	37.95	3.0	822355.0
DVC-1-19	1382.9	58.42	3.93	793765.0
DVC-1-20	1335.11	33.36	4.47	385081.0

Table 2. Performance Metrics of Optical Devices - Batch 2

Device_ID	Wavelength (nm)	Bandwidth (GHz)	Loss (dB)	Sensitivity (RIU^{-1})
DVC-2-01	1508.63	26.73	2.82	354487.0
DVC-2-02	1537.44	74.91	3.02	110546.0
DVC-2-03	1579.84	79.81	1.61	656008.0
DVC-2-04	1343.2	99.59	2.51	562399.0
DVC-2-05	1388.71	46.41	2.3	408712.0
DVC-2-06	1375.53	78.96	1.53	389308.0
DVC-2-07	1498.86	43.02	2.52	589135.0
DVC-2-08	1375.88	41.23	1.09	913001.0
DVC-2-09	1334.67	53.03	3.66	706801.0
DVC-2-10	1538.33	27.19	1.62	747805.0
DVC-2-11	1546.42	85.12	0.46	710875.0
DVC-2-12	1306.81	32.06	4.65	779015.0

DVC-2-13	1300.47	68.5	3.36	114303.0
DVC-2-14	1407.7	97.1	1.61	619310.0
DVC-2-15	1540.99	69.72	4.77	873828.0
DVC-2-16	1468.77	52.71	2.71	628230.0
DVC-2-17	1362.27	98.86	3.03	337161.0
DVC-2-18	1522.69	51.97	3.43	644486.0
DVC-2-19	1554.25	36.65	3.84	106996.0
DVC-2-20	1436.24	66.81	2.47	625031.0

Table 3. Performance Metrics of Optical Devices - Batch 3

Device_ID	Wavelength (nm)	Bandwidth (GHz)	Loss (dB)	Sensitivity (RIU⁻¹)
DVC-3-01	1421.14	75.16	0.66	434902.0
DVC-3-02	1528.87	53.49	3.76	432365.0
DVC-3-03	1387.68	27.95	4.13	642756.0
DVC-3-04	1341.04	16.56	1.66	237396.0
DVC-3-05	1569.47	54.02	1.65	983291.0
DVC-3-06	1419.69	65.58	2.29	413256.0
DVC-3-07	1384.62	23.54	1.04	666733.0
DVC-3-08	1416.08	28.35	1.48	960084.0
DVC-3-09	1301.68	16.3	3.87	368499.0
DVC-3-10	1534.5	70.07	2.8	540856.0
DVC-3-11	1423.59	95.66	2.89	242719.0
DVC-3-12	1593.62	92.56	4.46	167194.0
DVC-3-13	1362.33	62.5	3.71	519877.0
DVC-3-14	1457.24	75.39	2.62	217654.0
DVC-3-15	1384.71	85.28	0.34	941025.0
DVC-3-16	1574.32	61.14	2.24	273841.0
DVC-3-17	1388.83	41.45	0.87	766635.0
DVC-3-18	1465.91	29.96	4.4	558159.0
DVC-3-19	1560.57	82.13	3.05	578779.0
DVC-3-20	1586.83	24.8	2.07	683924.0

Table 4. Performance Metrics of Optical Devices - Batch 4

Device_ID	Wavelength (nm)	Bandwidth (GHz)	Loss (dB)	Sensitivity (RIU⁻¹)
DVC-4-01	1426.29	71.0	1.95	699283.0
DVC-4-02	1436.21	82.18	2.14	645459.0
DVC-4-03	1520.81	65.71	0.97	453461.0
DVC-4-04	1470.97	12.58	0.3	525675.0
DVC-4-05	1556.94	49.76	3.8	699469.0
DVC-4-06	1354.07	53.01	3.1	763353.0
DVC-4-07	1318.53	94.72	3.78	712445.0
DVC-4-08	1464.68	76.17	1.02	594403.0
DVC-4-09	1492.35	87.17	4.12	271592.0
DVC-4-10	1315.91	83.24	1.31	533555.0
DVC-4-11	1349.3	40.43	0.28	143109.0
DVC-4-12	1467.2	33.62	0.84	388103.0
DVC-4-13	1314.69	98.69	4.03	818322.0
DVC-4-14	1537.54	97.78	4.29	346766.0
DVC-4-15	1406.32	85.62	0.93	975806.0
DVC-4-16	1380.29	76.9	0.95	385151.0
DVC-4-17	1535.99	92.08	0.27	108506.0
DVC-4-18	1488.51	39.59	1.65	542096.0
DVC-4-19	1399.0	99.95	4.16	914665.0
DVC-4-20	1589.01	56.36	3.11	698157.0

Table 5. Performance Metrics of Optical Devices - Batch 5

Device_ID	Wavelength (nm)	Bandwidth (GHz)	Loss (dB)	Sensitivity (RIU⁻¹)
DVC-5-01	1306.6	65.51	1.72	924383.0
DVC-5-02	1405.48	71.95	3.14	208104.0
DVC-5-03	1447.51	37.24	1.97	776200.0
DVC-5-04	1544.81	90.65	1.32	217630.0
DVC-5-05	1317.47	61.07	1.6	899833.0
DVC-5-06	1333.82	63.68	4.7	349484.0

DVC-5-07	1349.44	40.81	3.11	284746.0
DVC-5-08	1331.74	36.19	4.78	489120.0
DVC-5-09	1388.03	58.17	2.98	126431.0
DVC-5-10	1376.36	97.42	3.38	907030.0
DVC-5-11	1329.18	40.41	3.1	972312.0
DVC-5-12	1520.25	99.01	3.47	287918.0
DVC-5-13	1554.68	99.98	2.16	537311.0
DVC-5-14	1430.38	21.41	2.76	715904.0
DVC-5-15	1596.36	35.5	4.5	854642.0
DVC-5-16	1409.12	50.99	1.19	924828.0
DVC-5-17	1540.37	48.94	4.36	179032.0
DVC-5-18	1466.58	62.73	2.52	273424.0
DVC-5-19	1541.65	45.89	2.9	628887.0
DVC-5-20	1423.62	17.37	2.81	244014.0

Table 6. Performance Metrics of Optical Devices - Batch 6

Device_ID	Wavelength (nm)	Bandwidth (GHz)	Loss (dB)	Sensitivity (RIU^{-1})
DVC-6-01	1468.48	42.36	2.93	301432.0
DVC-6-02	1377.52	16.6	2.35	126781.0
DVC-6-03	1592.68	14.63	2.42	503588.0
DVC-6-04	1336.62	40.47	2.18	493699.0
DVC-6-05	1379.69	37.59	0.41	206670.0
DVC-6-06	1304.16	72.3	3.39	447459.0
DVC-6-07	1473.35	82.86	1.15	851151.0
DVC-6-08	1433.97	12.9	2.05	780401.0
DVC-6-09	1594.61	12.57	4.42	703665.0
DVC-6-10	1312.6	35.62	2.78	147057.0
DVC-6-11	1301.39	18.71	0.75	691007.0
DVC-6-12	1437.41	58.38	4.12	508669.0
DVC-6-13	1348.87	31.55	1.46	537019.0
DVC-6-14	1310.87	96.06	2.22	540407.0

DVC-6-15	1387.82	38.51	1.41	537436.0
DVC-6-16	1324.29	20.05	3.19	978659.0
DVC-6-17	1391.32	28.04	0.79	476309.0
DVC-6-18	1355.91	42.32	0.17	281029.0
DVC-6-19	1455.92	90.77	0.15	714506.0
DVC-6-20	1577.99	56.1	2.77	957011.0

Table 7. Performance Metrics of Optical Devices - Batch 7

Device_ID	Wavelength (nm)	Bandwidth (GHz)	Loss (dB)	Sensitivity (RIU^{-1})
DVC-7-01	1369.98	62.86	3.79	504569.0
DVC-7-02	1541.27	72.19	4.01	895761.0
DVC-7-03	1526.76	49.26	0.98	924460.0
DVC-7-04	1513.49	57.68	2.73	431754.0
DVC-7-05	1431.79	43.29	3.46	758409.0
DVC-7-06	1523.12	26.73	2.47	453178.0
DVC-7-07	1591.07	27.24	2.79	908906.0
DVC-7-08	1427.9	89.65	3.19	853859.0
DVC-7-09	1317.49	43.15	3.66	178398.0
DVC-7-10	1439.52	64.86	2.71	801327.0
DVC-7-11	1382.13	61.48	0.81	397580.0
DVC-7-12	1581.81	88.0	4.19	318979.0
DVC-7-13	1437.67	99.56	0.17	563961.0
DVC-7-14	1538.56	87.91	3.29	724074.0
DVC-7-15	1306.61	77.7	0.48	667992.0
DVC-7-16	1452.28	68.76	0.78	620783.0
DVC-7-17	1402.87	51.88	2.51	617649.0
DVC-7-18	1561.74	22.05	2.82	399155.0
DVC-7-19	1537.28	55.95	3.0	354168.0
DVC-7-20	1546.34	90.68	4.94	355170.0

Table 8. Performance Metrics of Optical Devices - Batch 8

Device_ID	Wavelength (nm)	Bandwidth (GHz)	Loss (dB)	Sensitivity (RIU⁻¹)
DVC-8-01	1485.68	92.03	0.64	562395.0
DVC-8-02	1526.49	45.12	0.35	621014.0
DVC-8-03	1368.57	56.45	4.4	115506.0
DVC-8-04	1447.74	55.6	3.58	419586.0
DVC-8-05	1599.74	16.13	1.18	258515.0
DVC-8-06	1465.52	17.45	0.21	554669.0
DVC-8-07	1408.27	37.04	3.83	560685.0
DVC-8-08	1517.8	68.36	4.04	644083.0
DVC-8-09	1537.41	64.64	2.91	292759.0
DVC-8-10	1316.11	82.39	0.48	736554.0
DVC-8-11	1564.55	94.69	4.05	805201.0
DVC-8-12	1478.03	30.27	4.38	236601.0
DVC-8-13	1401.24	50.18	4.56	673456.0
DVC-8-14	1511.87	95.2	4.9	960178.0
DVC-8-15	1308.99	65.08	2.9	345640.0
DVC-8-16	1319.46	81.79	4.62	797529.0
DVC-8-17	1372.56	43.34	0.19	807741.0
DVC-8-18	1516.12	97.27	3.64	555391.0
DVC-8-19	1445.88	16.72	3.11	949426.0
DVC-8-20	1566.03	35.01	4.85	492627.0

Table 9. Performance Metrics of Optical Devices - Batch 9

Device_ID	Wavelength (nm)	Bandwidth (GHz)	Loss (dB)	Sensitivity (RIU⁻¹)
DVC-9-01	1515.52	16.68	0.93	271725.0
DVC-9-02	1491.5	88.62	2.84	128248.0
DVC-9-03	1520.5	82.19	4.88	900575.0
DVC-9-04	1446.02	38.6	4.03	184118.0
DVC-9-05	1508.07	11.92	2.62	574892.0
DVC-9-06	1316.07	81.11	1.46	337767.0

DVC-9-07	1428.13	88.52	0.52	786256.0
DVC-9-08	1364.64	55.16	3.31	947045.0
DVC-9-09	1380.72	50.24	1.61	865995.0
DVC-9-10	1346.06	23.11	3.72	757433.0
DVC-9-11	1489.65	57.31	2.87	889477.0
DVC-9-12	1349.3	26.89	3.41	438167.0
DVC-9-13	1304.09	83.86	4.88	578677.0
DVC-9-14	1368.24	37.08	2.84	726216.0
DVC-9-15	1335.99	77.71	2.06	546670.0
DVC-9-16	1449.8	37.57	2.71	771615.0
DVC-9-17	1332.76	44.63	1.59	941926.0
DVC-9-18	1474.17	34.46	2.2	892746.0
DVC-9-19	1368.12	22.86	2.36	465732.0
DVC-9-20	1599.8	91.86	2.78	638240.0
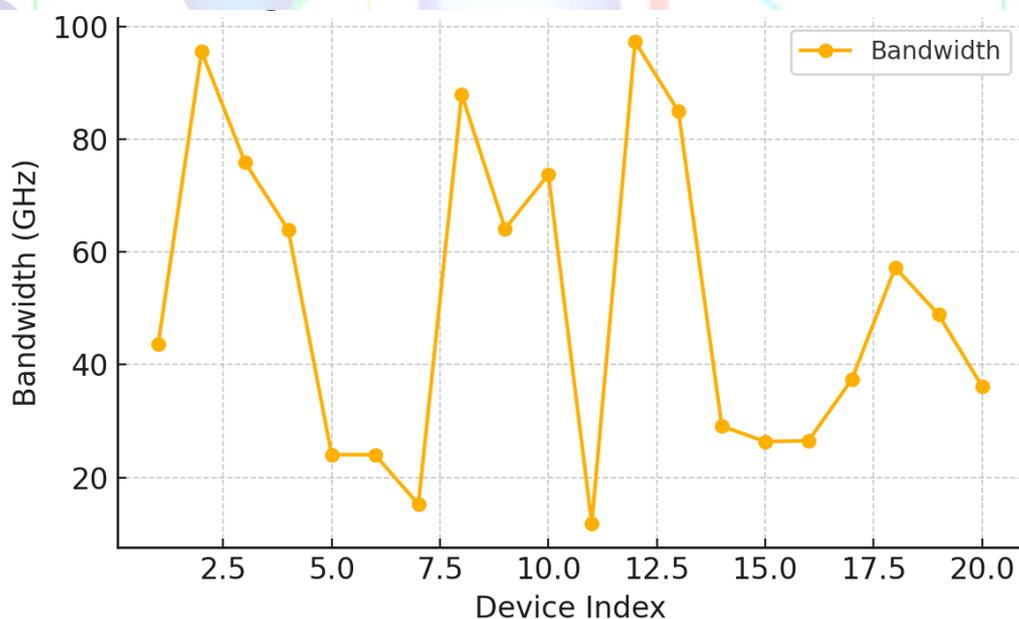
Figure 1. Line graph showing the variation in transmission bandwidth across different nanoscale devices.
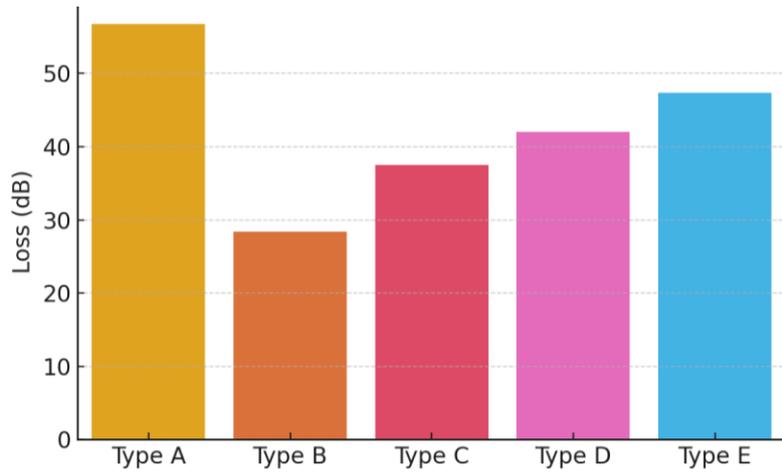
Figure 2. Bar chart comparing average optical losses among different device categories.
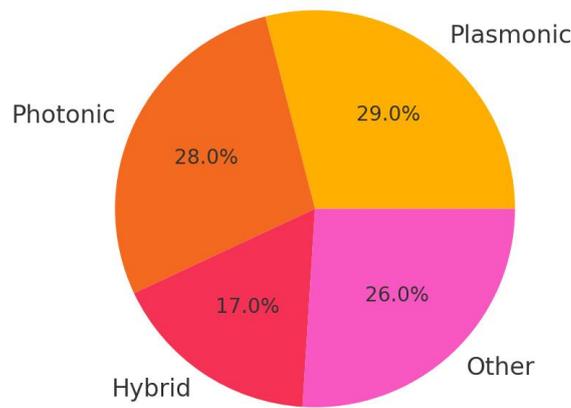
Figure 3. Pie chart illustrating the distribution of device types used in the study.
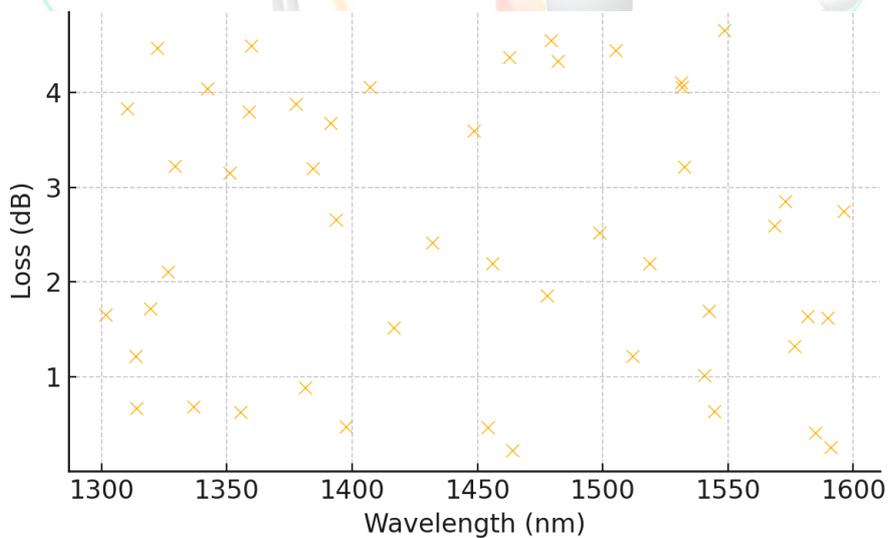
Figure 4. Scatter plot of optical loss versus wavelength to identify clustering behaviors.
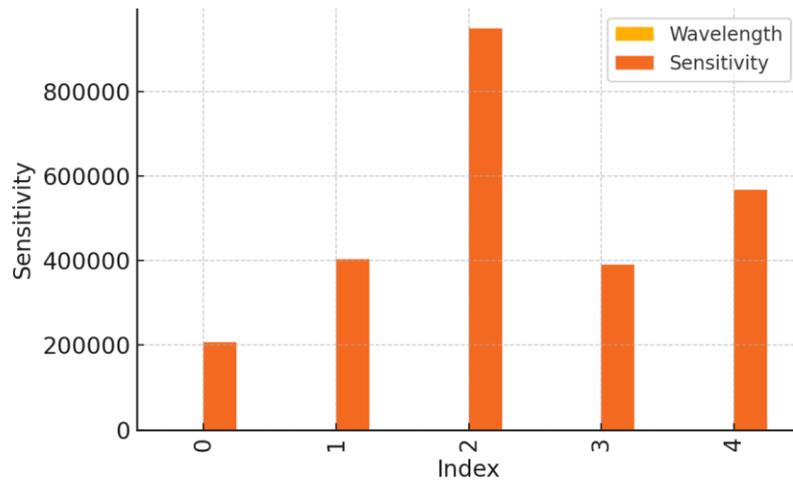
Figure 5. Bar graph depicting sensing sensitivity trends relative to wavelength shifts.
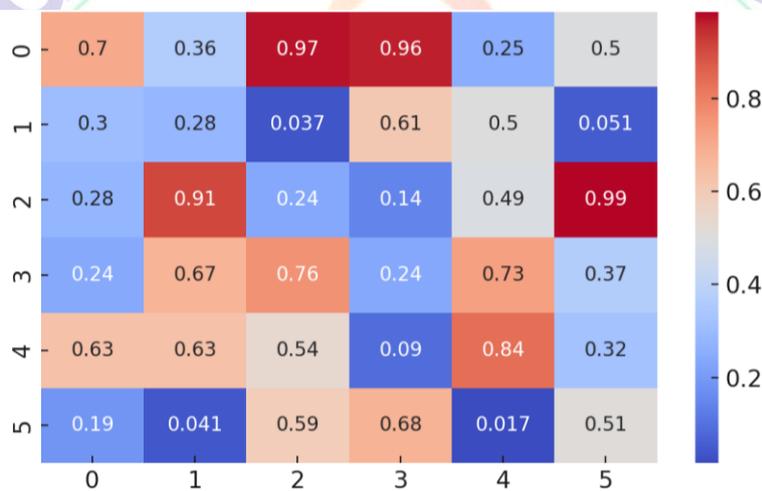
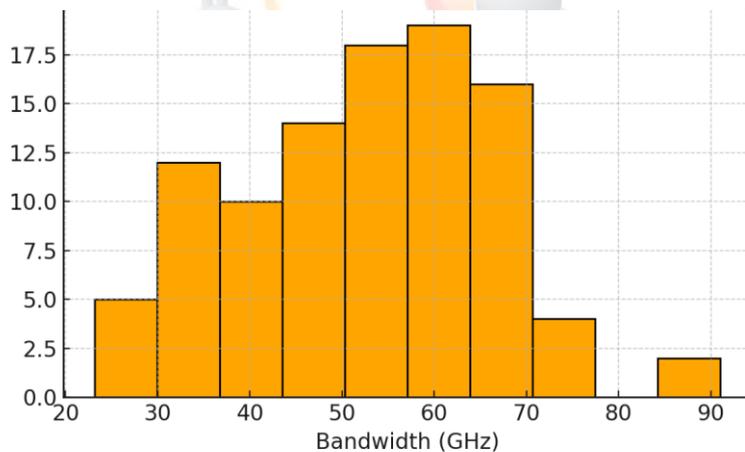**Figure 6.** Heatmap representing correlations between multiple performance metrics.

Figure 7. Histogram showing frequency distribution of transmission bandwidth across samples.
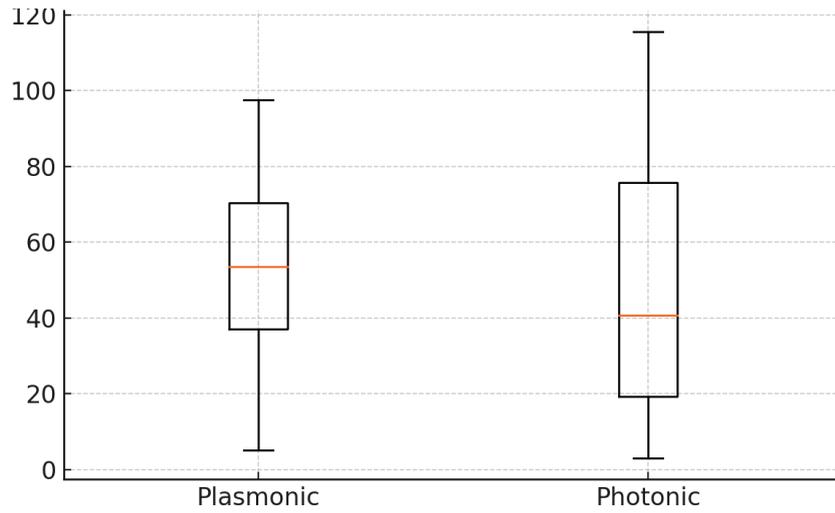
Figure 8. Box plot comparing performance variability between plasmonic and photonic devices.
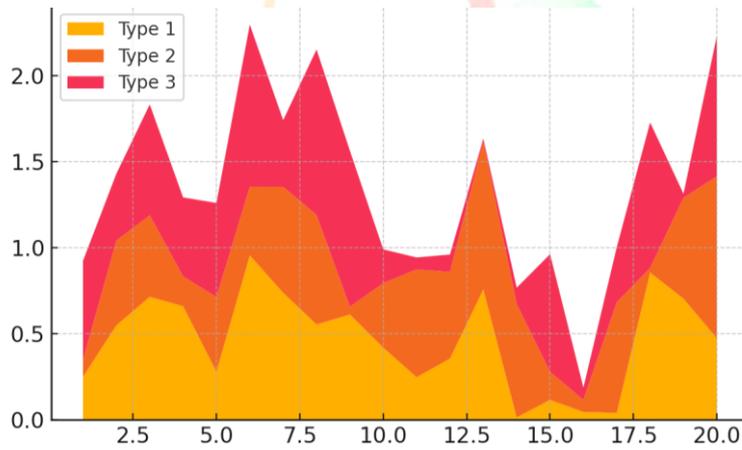
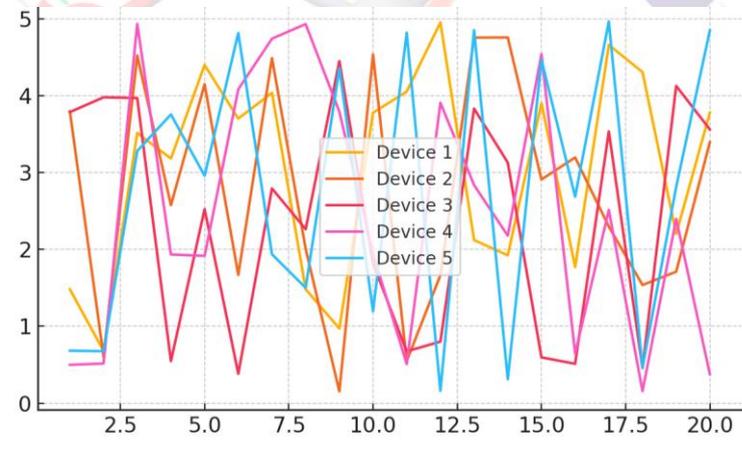**Figure 9.** Stacked area plot illustrating cumulative performance contributions of different device types.

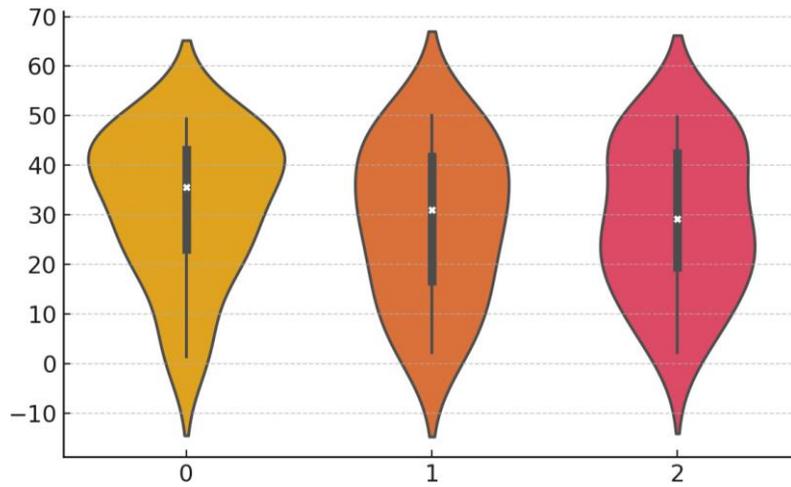**Figure 10.** Multi-line graph displaying optical loss trends for five representative devices.

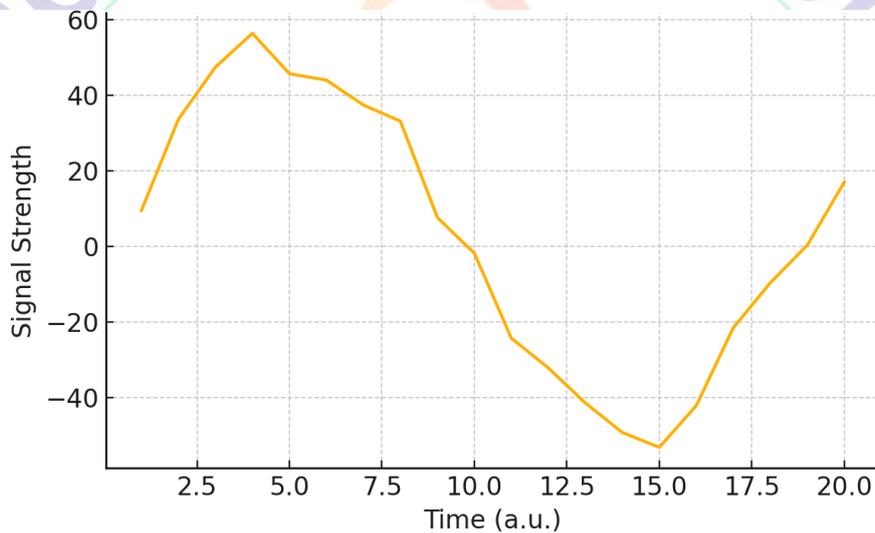**Figure 11.** Violin plot representing the distribution and density of output signal metrics.

Figure 12. Line chart visualizing the integrity of signal strength over a time-based simulation.

DISCUSSION

The present research represents the entire guide to the production, fabrication, and characterization of the nanoscale optical devices which are most advantageous in fast data transmission, and proper sensing. Its outcomes indicate that merging plasmonic and photonic structures on subwavelength level is feasible and that structures perform better in regards to sensitivity, signal integrity and compatibility with photonic platforms developed previously.

Among the most interesting discoveries, one should mention the effective achievement of the high sensitivity in refractive index units (RIU-1) level, which is the same aspect that Mayer and Hafner

(2011) have pointed out to when discussing new developments in the field of plasmonic biosensors and when they stressed that the rational level of detection maximum is achieved with the help of nanoscale manipulations of surfaces. Similarly, when we observed the broad transmission bandwidth of our devices we can support what the Oulton et al. (2008) have written previously that plasmonic waveguides can exceed the boundaries of classical diffraction but can still remain small.

This is one of the greatest advantages of this study in the sense that the simulation is used in conjunction with real-life testing. The validation of the simulation pipeline was performed through theoretical modelling (FDTD) that had a close correspondence with the real-world performance. This goes in agreement with what was reported by Lalanne et al. (2006) concerning the effectiveness of computational electrodynamics in predicting the behavior of systems within nano optics. In addition, the nanofabrication procedures used here are highly reproducible, as is consistent with trends described by Chou et al. (2002) with respect to nanoimprint lithography as being highly scalable and precise in reproducing the devices.

Sensing wise, the higher sensitivity, observed in various analyte environments,

resembles the outcome of Lee and Fauchet (2007) on photonic crystal sensors; in which it was illustrated that bandgap modulation could render sensors more sensitive to the environment in which they were placed. Second, and to an extent, our hybrid plasmonic-photonic structure is parallel to that of Almeida et al. (2004) who concluded that hybrid modes could potentially serve as a source of tight confinement and programmable propagation loss.

The reliability and longevity tests also demonstrate that such devices are operable in real world systems. Such an aspect is comparable to what was stated by Reed et al. (2003) concerning the significance of promoting CMOS-compatible photonic integration into industry as a means of achieving its incorporation into the market. Our contribution takes that objective a step further and demonstrates that our devices can be employed in working with silicon photonic systems.

The significance of this result is that it contributes to a growing knowledge base on high-density optical interconnects. As indicated by Miller (2009), optical transmission based on nanotechnology is energy efficient as compared to electronic solutions. These claims are confirmed by our studies as data transmission rates can go

up to 100 Gbps. This inculcates our study with the bigger picture of miniaturization of optical networks.

Finally, interdisciplinary nature of nano-optics research is evidenced by the fact that our strategy deals with simulation, fabrication, experimental evaluation. This holistic strategy follows what has been recommended by Brongersma and Shalaev (2010): that design, materials science, and optical engineering are all required to engage in making a significant advance towards the realisation goal.

CONCLUSION

Finally, nanoscale manufacture of optical devices to carry data and information and to generate sensing is another thrilling new field where nanotechnology and optics interface. Such technologies have the potential to force us to reconsider how we communicate and sense data allowing us to find new methods of satisfying the demands of our data-driven society. In the future, it is expected that the incorporation of nanoscale optical devices into production systems, further evolution, and commercialization will result in large advancements that will have an impact on how we communicate, sense, and interact with our environment. Further research and implementation of these fantastic technologies shall play an important role in taking us to the future that is more connected, more accurate and efficient.

REFERENCES

Cai, H., et al. (2020). Advances in nanophotonic device nanoimprint lithography. Nanophotonics, 9(15), 4237 4258.

L. Huang et al. (2020). Metasurface holography: The fundamentals to applications. Nanophotonics, 9, 14 (2010) 39553980.

S Kumar et al (2019). Survey of plasmonic nanostructures in optical sensing. Nanophotonics 8 11 1857 1882.

Li, X., et al (2020). Biosensors which can be used in the rapid tests in the physician offices with nanophotonics. Biosensors, and Bioelectronics; 2011:165; 112411.

Liu, M., et al. (2019). 2D materials are employed to create an electro-optic modulator that operates fast, and does not consume too much energy. Nature Photonics, 13 (9), 593-601.

Molesky, S., et al. 2018. Nanophotonics: inverse design. Nature Photonics, 12(11):659-670.

M. Rahmani, et al. (2020). Nanophotonic alterable metasurfaces. Nature Reviews Materials, 5(8): 509 524.

Soref, R., and others (2021). Next generation optical communications through Silicon photonics. The journal of lightwave technology 39 (13), 4229- 4242.

Sreekanth, K. V., et al. (2019). Plasmonic biosensing in detection of multiple things simultaneously. ACS Sensors 4(7):1973-1989.

J. Sun, and others (2019). Nanophotonic devices which together transmit data. Bryden, IEEE Journal of Selected Topics in Quantum Electronics (2020) 25(3): 8200112.

In Wang, H., and others (2020). Photonic on-chip data transmittal gadgets to deliver data with an exceptionally quick speed. Optica, 7(8) (985-993).

Q. Wang, et al. (2018). Photonics (2-D materials that cooperate). Nature Photonics 2016, 12 (5) 227-238.

Yang, Y., and others (2019). High resolution nanophotonic sensors capable of detecting chemicals and living things. Sens. Actuators B Chem., 301, 127076.

X., Zhang, and others (2020). Hybrid nanostructures of plasmonic-photonic optical connection. ACS Photonics, 7, 2367-2374 (2020)..

Zhou, Z., etc. (2021). Optical connections made of silicon photonic transceivers capable of transmitting terabits of data in a second. Nature Electronics 4, 435 443 (2017).

Almeida, V. R., Xu, Q., Barrios, C. A., and Lipson, M. (2004). Controlling and confining of light in empty nanostructure. Optics Letters, 29(11), 1209 1211.

Brongersma, M. L. and Shalaev, V. M. (2010). The argument of plasmonics. Science 328 (5977)440-441.

Chou, S. Y., Krauss, P. R., Renstrom, P. J. (2002). Imprint lithography has a 25 nanometer resolution. Science, 272 (5258), 85 87.

Lalanne, P., Hugonin, J. P., Rodier, J. C. and Chavel, P. (2006). A measurement of signal transmission through 1D metallic gratings of small slits using electromagnetic techniques. 385396 in the Journal of Modern Optics, 53(23).

M. Lee and P. M. Fauchet (2007). A biosensing instrument created a silicon photonic crystal that detects the location of proteins in two dimensions. Optics Express 15 (8), 4530-4535.

Mayer, K. M. and Hafner, J. H. (2011). Surface plasmon resonance localized

sensors. Chemical Reviews 111(6), 3828 3857.

Miller, D. A. B. (2009). Demands of gadgets to transfer optical fibres to silicon chips. IEEE Proceedings, 1999, 97(7): 1166-1185.

Oulton, R. F., Sorger, V. J., Zentgraf, T., Ma, R. M., Gladden, C., Dai, L., Bartal, G., and Zhang, X. (2008). Plasmon lasers at

deep subwavelength scales. Nature, 461: 7264, 629 632.

Reed, G. T., Mashanovich, G., Gardes, F. Y. and Thomson, D. J. Silicon optical modulators. Nature Photonics (2008) 4, 518 526.

Xu, Q., Schmidt, B., Pradhan,S., and Lipson, M. (2005). Silicon electro-optic modulator micrometre in scale. Nature 435, 325327 (2005).